J Mol Model (2014) 20:2467
DOI 10.1007/s00894-014-2467-2

ORIGINAL PAPER

Density functional study of molecular nitrogen adsorption on gold-copper and gold-silver binary clusters

Shuang Zhao · XinZhe Tian · JunNa Liu · YunLai Ren · JianJi Wang

Received: 19 July 2014 / Accepted: 14 September 2014 / Published online: 7 October 2014

Abstract Density functional theory calculations were performed to investigate the adsorption behaviors of nitrogen molecule on small bimetallic Au_nCu_m and Au_nAg_m clusters, with $n+m\leq5$. In all cases the N_2 forms a linear or quasi-linear M-N-N structure (M=Au, Cu or Ag). The adsorption energies of N_2 on pure metal clusters follow the order $Cu_nN_2>Au_nN_2>Ag_nN_2$, which is due to the weaker orbital interaction between silver and N_2. N_2 prefers to bind to a copper atom in $Au_nCu_mN_2$ complexes and prefers to bind to a silver atom in $Au_nAg_mN_2$ complexes. The combination of Cu atoms into Au_n clusters makes the cluster more reactive toward N_2 while the combination of Ag atoms into Au_n clusters makes the cluster less reactive toward N_2. The electrostatic interaction is strengthened while the back-donation from metal to N_2 is reduced in bimetallic cluster nitrides, as compared to the mono cluster nitrides. The N-N stretching frequencies are all red-shifted upon adsorption and the M-N stretching frequencies are highly correlated to the atoms to which the N is attached.

Keywords Bimetallic clusters · Density functional theory · Gold-Copper · Gold-Silver · Nitrogen adsorption

Introduction

Coinage metals (Au, Ag, and Cu) have similar electron configurations: a completely filled d shell and a singly occupied s shell, which can be seen as "alkali-like" metals [1]. In recent years, bimetallic coinage metal clusters have attracted considerable attention both experimentally and theoretically primarily because they often exhibit distinct physical and chemical properties from the pure coinage clusters [2–14]. The bimetallic Au/Cu nanoparticles confined in SBA-15 have much better performance than monometallic particles in catalyzing CO oxidation even with the presence of excess H_2 [11]. Pyridine prefers binding to silver when both silver and gold atoms co-exist at active sites of a mixed Au/Ag cluster [12]. Li et al. studied the small cationic $Au_nCu_m^+$ ($n+m\leq6$) clusters and their monocarbonyls $Au_nCu_mCO^+$ by first-principles calculations [13]. They found that CO prefers binding to Cu and the adsorption energy generally decreases with increasing Cu content in the mixed clusters, which is highly related to the electron transfer between CO and the cluster. Our previous theoretical study showed that the ionization potentials (IP), electron affinities (EA), and hydrogen adsorption energies of bimetallic Ag/Au cluster hydrides increase as the Au content increases [14].

The nanoparticles and clusters of coinage metal are good catalysts to reduce the toxic pollutants such as CO, NO_x, and hydrocarbons [15–22]. The reduction of NO_x with CO in the absence of oxygen yields N_2 as the main product [15–18]. The adsorption and desorption of N_2 on metal surface and clusters may play an important factor in understanding the catalytic mechanism. On the other hand, N_2 is isoelectronic with CO, and the same as CO, its highest occupied molecular orbital (HOMO) and lowest unoccupied molecular orbital (LUMO) are σ and π*, respectively. However, N_2 has bigger HOMO-LUMO gap, higher IP value and more negative EA than CO, which means it is more difficult for N_2 to give or draw electrons from metal cluster and will result in weaker interaction with metal clusters than CO [23]. The adsorption of CO on pure Au_n, Cu_n, Ag_n, and bimetallic Au/Ag, Au/Cu clusters has been extensively investigated and reported [13, 24–30]. In contrast, the available literature on the interaction of N_2 molecule with coinage metal cluster is limited to only one paper by Yang et al. to our

S. Zhao · X. Tian · J. Liu · Y. Ren · J. Wang (✉)
School of Chemical Engineering, Henan University of Science and Technology, Luoyang, Henan 471000, People's Republic of China
e-mail: jwang@htu.cn

knowledge [23]. It is found that the cationic Au_n^+ (n=1-6) and some neutral Au_n clusters (n=2-4) can adsorb N_2 molecule, while anionic Au_n^- can not [23]. In this contribution, we systematically investigate the interaction between N_2 molecule and small bimetallic Au_nCu_m and Au_nAg_m ($n+m\leq5$) clusters using the first principles methods on the basis of density functional theory (DFT). Our results presented below include three parts concerning geometries, adsorption energies, and frequency analysis, followed by a conclusion.

Computational details

The calculations were carried out using GAUSSIAN 09 package [31]. The PW91PW91 [32] exchange and correlation functional was employed for all the calculations in this study. The Stuttgart-Dresden effective core potential (ECP) plus DZ basis set [33] was used for Au, Ag, and Cu atoms. The 6-311++G(d,p) basis set was used on N atoms. The accuracy of this methodology for bimetallic Au/Cu and Au/Ag clusters has been tested in our previous work [14, 34]. All calculations were performed with (99,590) pruned grid (ultrafine grid as defined in Gaussian 09). Geometry optimization for the minima configuration occurred with all degrees of freedom and without any symmetry restriction. Natural bond orbital (NBO) [35] analysis was used to provide the natural charge distribution. The charge decomposition analysis (CDA) is performed following the work for constructing the wave function of the complex in terms of the linear combination of the donor and acceptor fragment orbitals (LCFO) [36, 37]. Vibrational frequency calculations including thermochemical analysis were carried out at 298.15 K and 1 atmosphere of pressure. These frequency calculations also guarantee the optimized structures locating the minima, not as transition structures.

Results and discussion

Structures and stabilities

To have the results of bare clusters and complex clusters for comparison, we first optimized the geometries of bare Au_nCu_m and Au_nAg_m clusters with $n+m\leq5$. The most stable Au_nCu_m and Au_nAg_m clusters taken from our previous work [13, 38] are displayed in Figs. 1 and 2, respectively. It can be observed that the Au_nCu_m and Au_nAg_m clusters have similar structures in which the Au atoms prefer exposed positions while the Cu or Ag atoms form a higher number of bonds. Such topologies are convenient for electron transfer from Cu or Ag to Au and easily reduce geometrical reconstruction. The geometries of Au_nCu_m and Au_nAg_m clusters according to PW91PW91 calculations are consistent with previous theoretical reports [3–6].

The structures of the most stable $Au_nCu_mN_2$ and $Au_nAg_mN_2$ complexes are displayed in Figs. 3 and 4, respectively (more structures can be seen in the Supporting information for the conciseness of the text). The degree of M-N-N angle and the CDA results are listed in Tables 1 and 2. The metal frameworks, in both $Au_nCu_mN_2$ and $Au_nAg_mN_2$, retain their overall shape when N_2 is attached in most cases and even the bond distances between metal atoms changed by less than 0.05 Å. Moreover, most M-M* bonds (asterisk denotes the atom of the adsorption site on the metal cluster) are slightly elongated and only a few M-M bonds far from N_2 molecule are shortened to some extent. With the exception of $Au_2Cu_3N_2$, all the complexes prefer planar structures. Similar situation can also be seen in previous theoretical works of CO, NO_x, and H atoms adsorption on small binary gold-alloy clusters and no well supported explanation is given [14, 28, 38, 39]. One important consensus is that the reason for the planar structures may be attributed to the strong scalar relativistic effects of Au atoms [40–42].

From Fig. 3 it can be observed that in all cases of $Au_nCu_mN_2$, N_2 molecular bonds to metal clusters by one

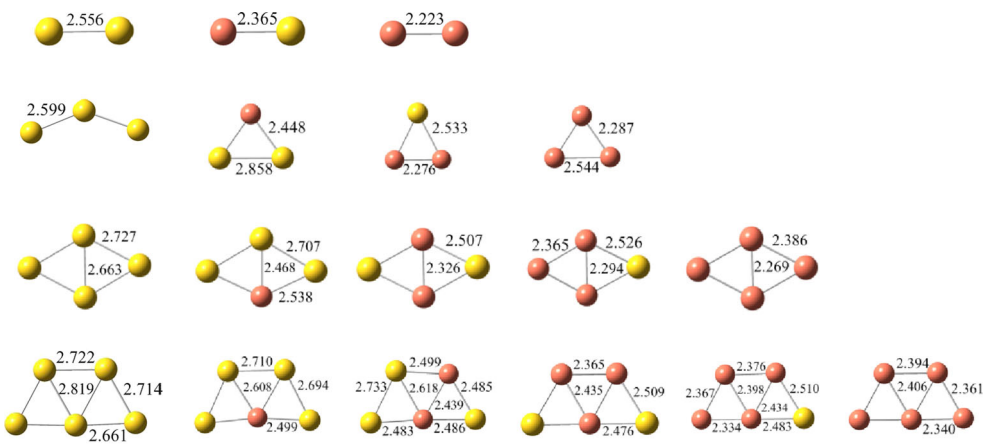

Fig. 1 Optimized geometries of the most stable Au_nCu_m clusters, with n+m≤5. The structures are arranged in the order of increasing Cu composition. All the lengths marked are in Å. The Au and Cu atoms are shown in yellow and *red*, respectively

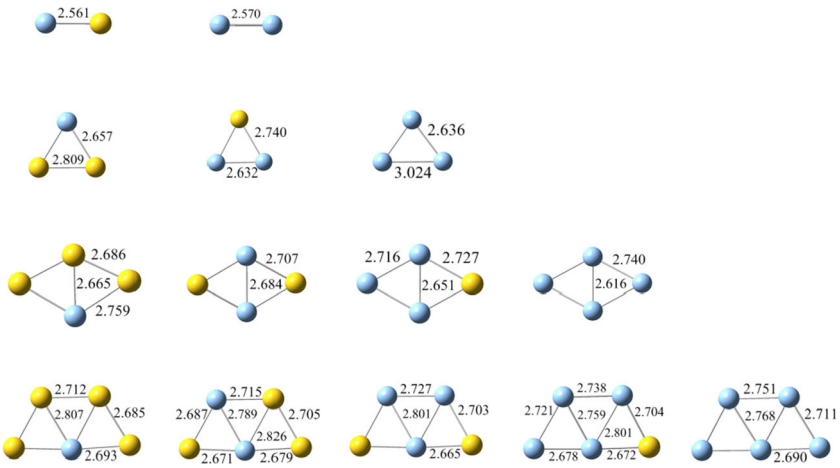

Fig. 2 Optimized geometries of the most stable Au_nAg_m clusters, with n+m≤5. The structures are arranged in the order of increasing Ag composition. All the lengths marked are in Å. The Au and Ag atoms are shown in *yellow* and light *blue*, respectively

metal-N bond, and forms a linear or quasi-linear M-N-N geometry (170.5-180.0°), which is similar to the cases of N_2 adsorption on W_n (n≤5) [43] and Mo_n (n=2-8) clusters [44]. The only exception is Au_5N_2 where the Au-N-N angle is 156.2°. In the gas-phase, the calculated N-N distance is 1.106 Å, in good agreement with the experimental value of 1.098 Å [45]. The N-N distance is slightly elongated upon adsorption. The N-N distance in Cu_nN_2 complexes changes from 1.117 to 1.122 Å, which is a little longer than that in Au_nN_2 complexes (1.113 to 1.116 Å), indicating that the lengthening of N-N bond is more apparent in Cu_nN_2. The Au-N distance ranges from 2.036 to 2.200 Å in Au_nN_2 complexes, while the Cu-N distances ranges from 1.842 to 1.895 Å in Cu_nN_2 complexes. The lanthanide contraction makes the gold atom have a close covalent radius to that of copper atom. If the difference of Au-N and Cu-N distance is due to the bonding interaction, we can see that in all the cases the Cu-N bond is stronger than the Au-N bond, which is also supported by the larger adsorption energies of Cu_nN_2 than Au_nN_2. The N_2 molecule prefers binding to Cu when both Au and Cu sites co-exist in the bimetallic $Au_nCu_mN_2$ clusters. The N-N and Cu-N distances in bimetallic $Au_nCu_mN_2$ complex range from 1.115 to 1.120 Å and 1.830 to 1.891 Å, respectively, which are slightly shorter than the corresponding values in mono Cu_nN_2.

The calculations do not predict any marked structural relaxations of Au_nCu_m clusters upon N_2 adsorption. In all cases, the lowest-energy structures of $Au_nCu_mN_2$ are related to the ground state isomers of bare Au_nCu_m. However, there are two exceptions of Au_4CuN_2 and $Au_2Cu_3N_2$. In Au_4CuN_2, although the isomer with Cu three-coordinated is 0.13 eV higher in energy than the ground state with Cu four-coordinated, the adsorption of N_2 on the less stable isomer leads to the most stable Au_4CuN_2. Similarly, the most stable $Au_2Cu_3N_2$ was

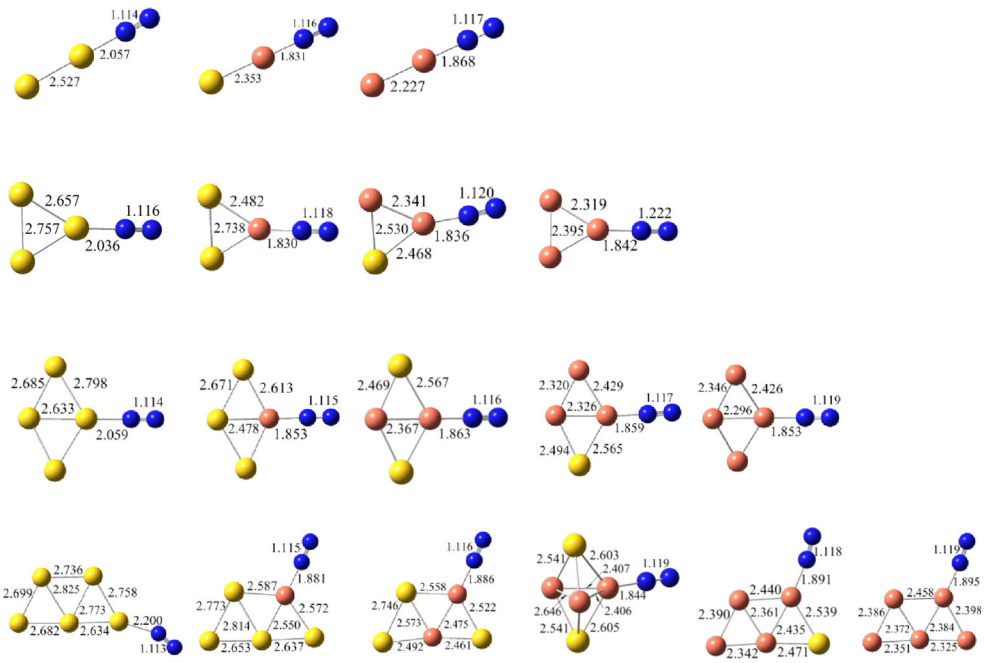

Fig. 3 Optimized geometries of the most stable $Au_nCu_mN_2$ clusters, with n+m≤5. The structures are arranged in the order of increasing Cu composition. All the lengths marked are in Å. The Au, Cu, and N atoms are shown in *yellow*, *red* and *navy blue*, respectively

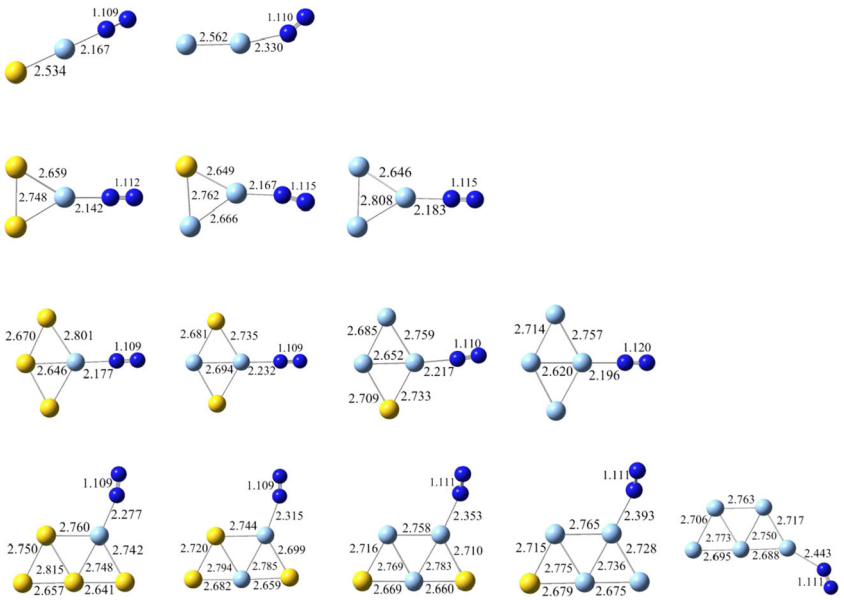

Fig. 4 Optimized geometries of the most stable $Au_nAg_mN_2$ clusters, with n+m≤5. The structures are arranged in the order of increasing Ag composition. All the lengths marked are in Å. The Au, Ag, and N atoms are shown in *yellow*, *light blue*, and *navy blue*, respectively

not obtained by binding of N_2 molecule to the most stable Au_2Cu_3 with C_{2v} symmetry, but was obtained by binding of N_2 on the less stable trigonal bipyramid with D_{3h} symmetry.

The most stable $Au_nAg_mN_2$ complexes are shown in Fig. 4. The geometries of the metal frameworks in $Au_nAg_mN_2$ are very similar to bare Au_nAg_m clusters except for Au_4AgN_2. In $Au_nAg_mN_2$ complex, the N_2 molecule always binds to an Ag atom when it is available. The N-N distance changes from 1.109 to 1.115 Å. The Ag-N distance in $Au_nAg_mN_2$ changes from 2.142 to 2.443 Å, which is longer than both the Au-N and Cu-N distances discussed above. It should be noted that in some cases of $Au_nAg_mN_2$ there is a linear M-N-N geometry while in other cases there is a bent angle of M-N-N axis. The electron transfer from the filled σ orbital of N_2 to the metal (donation) and the electron transfer from the occupied orbitals of the transition metal to the empty π* orbitals of N_2 (back-donation) are the two important mechanisms in the interaction

Table 1 Bond angle of M-N-N (in degree, M=Au or Cu), and charge decomposition analysis (in e) of the most stable $Au_nCu_mN_2$ complex, with n+m≤5 (donation d, back-donation b)

Species	Angle (M-N-N)	d	b	d-b
Au_2N_2	179.9	0.131	0.017	0.114
$AuCuN_2$	179.9	0.123	0.034	0.088
Cu_2N_2	180.0	0.140	0.036	0.105
Au_3N_2	179.5	0.109	0.019	0.090
Au_2CuN_2	180.0	0.120	0.047	0.073
$AuCu_2N_2$	175.1	0.121	0.039	0.082
Cu_3N_2	179.9	0.132	0.045	0.086
Au_4N_2	179.9	0.127	0.022	0.105
Au_3CuN_2	179.9	0.146	0.043	0.103
$Au_2Cu_2N_2$	179.9	0.151	0.045	0.106
$AuCu_3N_2$	178.5	0.150	0.046	0.103
Cu_4N_2	180.0	0.150	0.047	0.103
Au_5N_2	156.2	0.153	0.020	0.133
Au_4CuN_2	176.5	0.148	0.033	0.115
$Au_3Cu_2N_2$	176.5	0.148	0.037	0.111
$Au_2Cu_3N_2$	180.0	0.138	0.060	0.078
$AuCu_4N_2$	170.5	0.149	0.037	0.112
Cu_5N_2	172.3	0.149	0.033	0.116

Table 2 Bond angle of M-N-N (in degree, M=Ag), and charge decomposition analysis (in e) of the most stable $Au_nAg_mN_2$ complex, with n+m≤5 (donation d, back-donation b)

Species	Angle (Ag-N-N)	d	b	d-b
$AuAgN_2$	180.0	0.158	0.017	0.141
Ag_2N_2	147.4	0.145	0.022	0.123
Au_2AgN_2	180.0	0.147	0.020	0.127
$AuAg_2N_2$	166.0	0.151	0.020	0.131
Ag_3N_2	179.6	0.152	0.019	0.134
Au_3AgN_2	179.9	0.156	0.020	0.136
$Au_2Ag_2N_2$	180.0	0.156	0.020	0.136
$AuAg_3N_2$	176.0	0.150	0.046	0.103
Ag_4N_2	179.9	0.121	0.023	0.138
Au_4AgN_2	161.3	0.160	0.017	0.143
$Au_3Ag_2N_2$	160.8	0.158	0.017	0.141
$Au_2Ag_3N_2$	151.9	0.157	0.020	0.138
$AuAg_4N_2$	147.7	0.154	0.020	0.134
Ag_5N_2	141.5	0.153	0.020	0.132

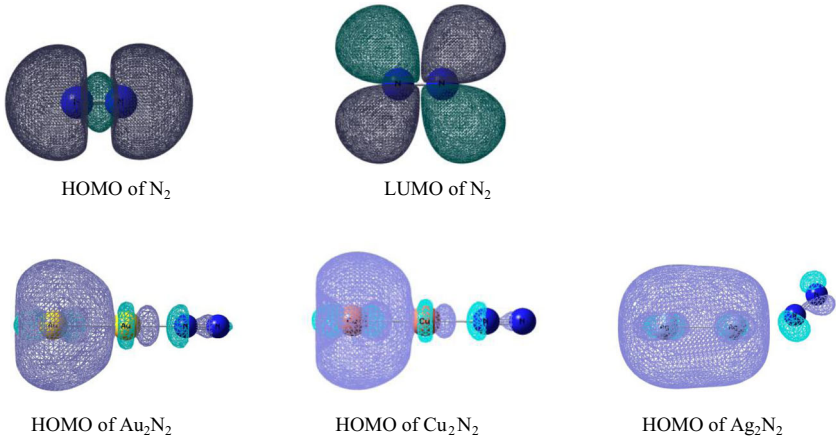

Fig. 5 HOMO and LUMO orbitals for N_2 molecule, and HOMO orbitals for Au_2N_2, Cu_2N_2 and Ag_2N_2

between N_2 and metal cluster. The results of the charge decomposition analysis (CDA) also confirm the donation and back-donation mechanisms of the bonding of N_2 to the cluster. For this analysis we considered metal framework and N_2 as the two fragments. There is in fact a donation ranging from 0.109 to 0.161*e* from the N_2 to metal cluster and a back-donation ranging from 0.017 to 0.060*e* from metal cluster back to N_2. However, the larger electron transfer of donation should not be considered as evidence that the ligand-to-metal donation is stronger than the back-donation [36]. The relative magnitude of the two contributions has been discussed controversely in the past [46–50]. Figure 5 displays the σ (HOMO) and π*(LUMO) orbitals of the N_2 molecule, the HOMO orbitals of Au_2N_2, Cu_2N_2, and Ag_2N_2. It seems that in Ag_2N_2 the back-donation is more important, which leads to the bending of the Ag-N-N axis for the better overlap between the orbitals, while in Au_2N_2 and Cu_2N_2, the donation interaction is more important, which results in the linear M-N-N formation. The competition of the donation and back-donation process responsible for the linear or bent M-N-N axis has been fully interpreted in the previous theoretical study of N_2 adsorption on neutral and charged Au_n clusters with $n \leq 6$ [23].

Adsorption energies

The adsorption energy of N_2 is defined by the follow equation:

$$AE = E_{\text{bare cluster}} + E_{N_2} - E_{\text{complex cluster}},$$

where $E_{\text{bare cluster}}$ and $E_{\text{complex cluster}}$ are the total energies of the bare cluster and the complex cluster, respectively. The more positive the AE is, the stronger the bond. All adsorption energies were corrected with basis set superposition error (BSSE) estimated by using the counterpoise corrections method [51].

In Fig. 6, the adsorption energies as a function of cluster size for mono Au_nN_2, Cu_nN_2, and Ag_nN_2 are plotted. The AEs of Au_nN_2 decrease as the cluster size grows. For Cu_nN_2 and Ag_nN_2, the AE is the lowest at $n=5$ while it peaks at $n=3$. As seen from Fig. 6, the adsorption energies of N_2 follow the order $Cu_nN_2 > Au_nN_2 > Ag_nN_2$ with the same n. Similarly, the adsorption energies between Ag_n cluters and CO are smaller than their copper and gold counterparts [24–26, 29]. As for group 11 metals, the orbitial interactions with CO are smallest

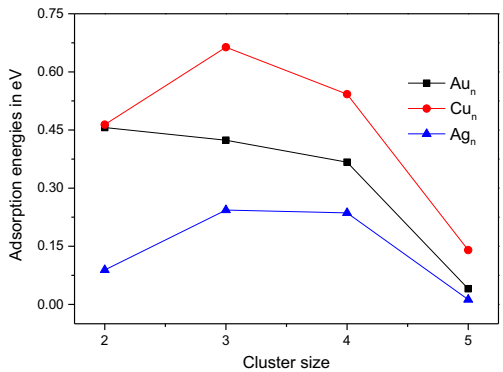

Fig. 6 Adsorption energies versus the cluster size for Au_nN_2, Cu_nN_2, and Ag_nN_2, with $n \leq 5$

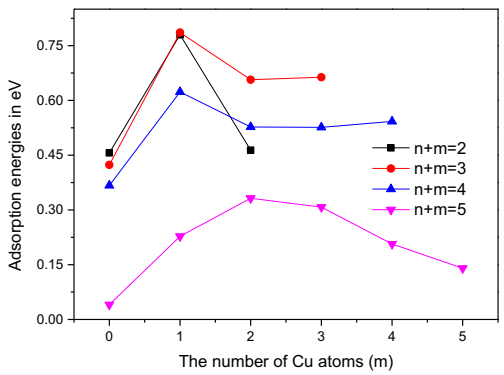

Fig. 7 Adsorption energies versus the contents of Cu atoms for $Au_nCu_mN_2$ clusters, with $n+m \leq 5$

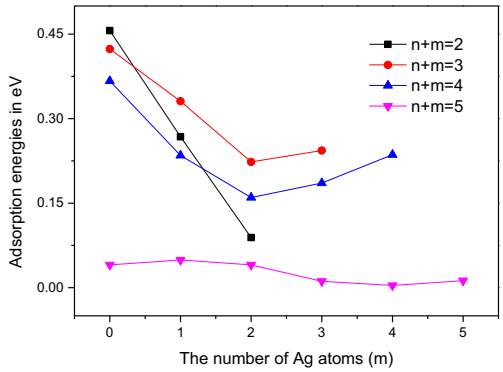

Fig. 8 Adsorption energies versus the contents of Ag atoms for $Au_nAg_mN_2$ clusters, with $n+m\leq5$

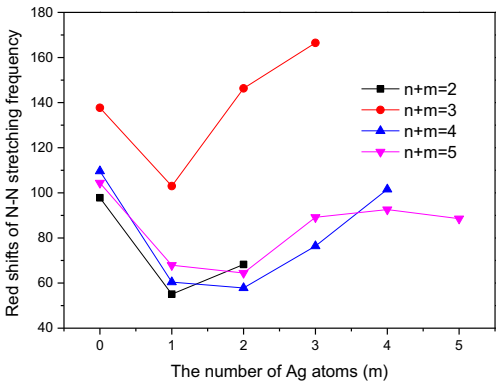

Fig. 10 *Red shifts* of N-N stretching frequencies versus the contents of Ag atoms for $Au_nAg_mN_2$ clusters, with $n+m\leq5$

for Ag [52]. N_2 and CO are isoelectronic and their molecular orbital are similar to each other. Thus the orbital interactions between metal atomic orbitals and N_2 frontier orbitals may have similar feature as CO. At the PW91PW91/SDD level, the energy levels of the valence *d* and *s* orbitals are −0.191 and −0.185 au for Cu atom, −0.262 and −0.225 au for Au atom. Compared with Cu and Au, the energy difference between *d* and *s* orbitals of Ag is much larger (−0.275 and −0.179au). It can be seen that there is a better energy match between the Cu 3*d* orbitals and the π* orbitals of N_2 (−0.079 au) and a better energy match between the Au 6*s* orbital and the σ orbital of N_2 (−0.381 au), while the energy combination for both donation and back-donation is the least favorable for Ag. In the clusters, it is then expected that Cu_n has the highest *d* band orbitals and Au_n has the lowest *s* band orbitals for the clusters with the same *n*. Therefore, in Cu_nN_2 complexes the back-donation interaction is stronger and in Au_nN_2 complexes the donation interaction is stronger, while both the donation and back-donation are the weakest in Ag_nN_2. As a consequence, the adsorption energies for Ag_nN_2 are usually much smaller than Cu_nN_2 and Au_nN_2 with the same *n*.

The adsorption energies for bimetallic $Au_nCu_mN_2$ and $Au_nAg_mN_2$ complexes are plotted in Fig. 7 and 8, respectively. Like the case of mono-meal nitrides, generally the AEs of $Au_nCu_mN_2$ and $Au_nAg_mN_2$ decrease as the cluster size

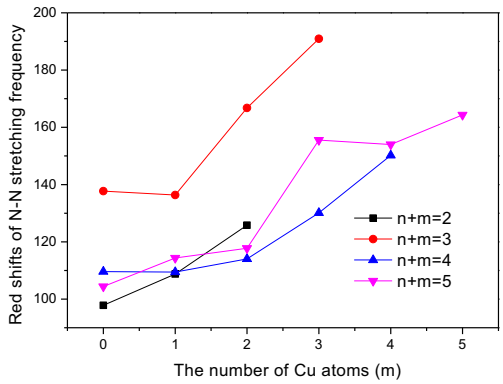

Fig. 9 *Red shifts* of N-N stretching frequencies versus the contents of Cu atoms for $Au_nCu_mN_2$ clusters, with $n+m\leq5$

increases. As discussed above, the AE for Cu_nN_2 complexes is larger than that of Au_nN_2, while the AE for Ag_nN_2 complexes is smaller than that of Au_nN_2. Thus we may expect that the dope of Cu in Au_n clusters tends to increase the AEs while the dope of Ag in Au_n tends to decrease the AEs with respective to pure Au_n. Indeed, as shown in Figs. 7 and 8, the AEs of bimetallic Au_nCu_m clusters are all larger than the AEs of pure Au clusters while the AEs for the bimetallic Au_nAg_m clusters are all smaller than the AEs of pure Au clusters with the exception of $n+m=5$.

Furthermore, the AEs of bimetallic Au_nCu_m pentamers ($n+m=5$) are even larger than Cu_5 cluster. The AE is especially enhanced on the alloy Au_nCu_m clusters with only one Cu atom compared to the pure Cu_n or Au_n clusters with $n+m=2$, 3, and 4. These results indicate that the alloying of Au and Cu can increase the reactivity of clusters toward N_2 with respect to pure Au_n or Cu_n clusters in some cases. Because Au is more electronegative than Cu, Au will draw some electron density at the expensive of Cu in a mixed Au/Cu cluster. The positive charge on the Cu atom connected to N in $Au_nCu_mN_2$ is much larger than that in Cu_nN_2, especially in bimetallic Au/Cu clusters with only one Cu atom doped. For example, the positive charge on the Cu atom connected to N in Au_2CuN_2 is +0.245*e*, compared with +0.064*e* in Cu_3N_2. As a consequence, the electrostatic interactions between the positive charged $Cu^{\delta+}$ connected to N and the lone pair of N_2 become more significant in bimetallic $Au_nCu_mN_2$ than mono Cu_nN_2 and Au_nN_2 clusters. On the other hand, the more positively charged $Cu^{\delta+}$ in bimetallic clusters may reduced the π back-donation from the metal to the empty N_2 orbital (π*). We performed an energy decomposition analysis (EDA) of the interaction between metal framework and N_2 on Cu_3N_2 and Au_2CuN_2 clusters. The orbital contribution to the interaction energy is increased by about 13 kJ mol^{-1} while the steric contribution consisting of both the electrostatic and exchange repulsion energies is decreased by about 17 kJ mol^{-1} from Cu_3N_2 to Au_2CuN_2. The larger AEs of $Au_nCu_mN_2$ than their corresponding Cu_nN_2 counterparts with the same cluster size may be attributed to that in these complexes the electrostatic

effects on the Cu-N bonds are much stronger than the effects of the reduction of π back-donation. Compared with $Au_nCu_mN_2$, the positive charges on Ag atoms in $Au_nAg_mN_2$ are smaller than those on Cu atoms, which leads to weaker coulombic attractions in $Au_nAg_mN_2$. It seems that in $Au_nAg_mN_2$ the electrostatic interaction is not as important as donation and back-donation interactions. For bimetallic $Au_nAg_mN_2$ with $n+m=3$ and 4 the AE gets its valley at $m=2$. This may indicate that the π back-donation is significantly reduced in these complexes. For $Au_nAg_mN_2$ with $n+m=5$ the largest AE occurs at Au_4Ag. However, the curve of pentamer is rather smooth and all the calculated AEs are less than 0.05 eV. These calculated AEs of pentamers are within the computational errors and indicated that the N_2 may not be adsorbed on bimetallic Au/Cu pentamers. Overall, it seems that it is difficult to separate the effects of various factors stated above and accurate predictions of the changes of AEs continue to be a challenging work.

Frequency analysis

In this adsorption system, we have calculated the vibrational frequencies for all the complex clusters studied above. The Cu-N bonds possess higher stretching frequencies (324-407 cm^{-1}) than both the Au-N (193-301 cm^{-1}) and the Ag-N (188-249 cm^{-1}) stretching frequencies. The calculated N-N frequency for the isolated N_2 is 2354 cm^{-1}, which is in good agreement with the experimental value of 2359 cm^{-1} [45]. Substantial red shifts of N-N stretching frequencies can be observed upon N_2 adsorption on metal clusters. For $Au_nCu_mN_2$ and $Au_nAg_mN_2$ complex the red shifts of N-N stretching frequencies are plotted in Figs. 9 and 10, as a function of Cu and Ag composition, respectively. In $Au_nCu_mN_2$ generally the red shifts increase as the Cu content increases for the given cluster size. In $Au_nAg_mN_2$, the N-N frequency is shifted the least when $m=1$ for dimer and trimer, while when $m=2$ for tetramer and pentamer. It is not surprising that there is no direct correlation between the N-N frequency and the adsorption energy because these two quantities are the reflection of two different bonding environments. The N-N frequency is a direct consequence of the N-N bonding, whereas the adsorption energy is the consequence of the metal atom and N bonding. Similarly, the N-N frequency does not correlate well with the NBO charge on adsorbed N_2 probably due to the very complicated electron density transfer processes during N_2 adsorption (donation and back-donation).

Conclusions

In this paper, the adsorptions of N_2 molecule on bimetallic Au/Cu and Au/Ag clusters up to five metal atoms were investigated by use of DFT. Our results indicate that the bimetallic metal clusters can adsorb N_2 molecule with the exception of Au/Ag pentamers. Adsorption of N_2 on pure Ag_n clusters is generally weaker than that on the copper and gold counterparts with the same cluster size. This is because both σ donation and π back-donation are the smallest for Ag. In the optimized geometries of $Au_nCu_mN_2$ and $Au_nAg_mN_2$, the N_2 molecule always binds to a copper atom or a silver atom, when it is available. The alloying of Au and Cu increases the adsorption energies with respect to pure Au_n, even with respect to pure Cu_n clusters in some cases. In contrast, the alloying of Au and Ag decreases the adsorption energies with respect to pure Au_n clusters. This may be attributed to that electrostatic effect is more significant in $Au_nCu_mN_2$ complex than that in $Au_nAg_mN_2$ complex. The M-C frequencies are related to atoms (Au, Cu or Au) to which the N is attached. The red-shift of N-N frequencies generally increases as the Cu content increases in $Au_nCu_mN_2$ for the given cluster size, while it reaches local minimum at m=1 or 2 in $Au_nAg_mN_2$. This study has provided a more complete understanding of the interaction between nitrogen molecule and metal clusters.

Acknowledgments This work was supported by the National Natural Science Foundation of China (Grant No. 21,133,009 and No. 21,002,023).

References

1. Ervin KM (2001) Metal-ligand interactions: gas-phase transition metal cluster carbonyls. Int Rev Phys Chem 20:127–164
2. Zhang H, Zelmon DE, Deng L, Liu HK, Teo BK (2001) Optical limiting behavior of nanosized polyicosahedral gold-silver clusters based on third-order nonlinear optical effects. J Am Chem Soc 123: 11300–11301
3. Lee HM, Ge M, Sahu BR, Tarakeshwar P, Kim KS (2003) Geometrical and electronic structures of gold, silver, and gold-silver binary clusters: origins of ductility of gold and gold-silver alloy formation. J Phys Chem B 107:9994–10005
4. Wang HQ, Kuang XY, Li HF (2010) Density functional study of structural and electronic properties of bimetallic copper-gold clusters: comparison with pure and doped gold clusters. Phys Chem Chem Phys 12:5156–5165
5. Zhao YR, Kuang XY, Zheng BB, Li YF, Wang SJ (2011) Equilibrium geometries, stabilities, and electronic properties of the bimetallic M_2-doped Au_n (M=Ag, Cu; n=1–10) clusters: comparison with pure gold clusters. J Phys Chem A 115:569–576
6. Kuang X, Wang X, Liu G (2011) Structural, electronic and magnetic properties of small gold clusters with a copper impurity. Trans Met Chem 36:643–652
7. Jiang ZY, Lee KH, Li ST, Chu SY (2006) Structures and charge distributions of cationic and neutral $Cu_{n-1}Ag$ clusters (n=2-8). Phys Rev B 73:235423
8. Lou XH, Gao H, Wang WZ, Xu C, Zhang H, Zhang ZJ (2010) A theoretical study of the atomic hydrogen binding on small Ag_nCu_m ($n+m\leq5$) clusters. J Mol Struct (Theochem) 959:75–79
9. Zhao S, Lu WW, Ren YL, Wang JJ, Yin WP (2012) Density functional study of cationic and anionic Ag_mCu_n ($m+n\leq5$) clusters. Commun Theor Phys 57:452–458

10. Joshi AM, Delgass WN, Thomson KT (2006) Analysis of O_2 adsorption on binary-alloy clusters of gold: energetics and correlations. J Phys Chem B 110:23373–23387
11. Liu X, Wang A, Wang X, Mou CY, Zhang T (2008) Au-Cu alloy nanoparticles confined in SBA-15 as a highly efficient catalyst for CO oxidation. Chem Commun 27:3187–3189
12. Wu DY, Ren B, Tian ZQ (2006) Binding interactions and Raman spectral properties of pyridine interacting with bimetallic silver-gold clusters. ChemPhysChem 7:619–628
13. Zhao Y, Li Z, Yang J (2009) A density functional study on cationic $Au_nCu_m^+$ clusters and their monocarbonyls. Phys Chem Chem Phys 11:2329–2334
14. Zhao S, Ren YL, Wang J, Yin WP (2010) Density functional study of hydrogen binding on gold and silver-gold clusters. J Phys Chem A 114:4917–4923
15. Arve K, Adam J, Simakova O, Capek L, Eranen K, Murzin DY (2009) Selective catalytic reduction of NO_x over nano-sized gold catalysts supported on alumina and titania and over bimetallic gold-silver catalysts supported on alumina. Top Catal 52:1762–1765
16. Bin F, Song CL, Lv G, Song JO, Wu SH, Li XD (2014) Selective catalytic reduction of nitric oxide with ammonia over zirconium-doped copper/ZSM-5 catalysts. Appl Catal B 150:532–543
17. Kameoka S, Ukisu Y, Miyadera T (2000) Selective catalytic reduction of NO_x with CH_3OH, C_2H_5OH and C_3H_6 in the presence of O_2 over Ag/Al_2O_3 catalyst: Role of surface nitrate species. Phys Chem Chem Phys 2:367–372
18. Ueda A, Haruta M (1999) Nitric oxide reduction with hydrogen, carbon monoxide, and hydrocarbons over gold catalysts. Gold Bull 32:3–11
19. Valden M, Lai X, Goodman DW (1998) Onset of catalytic activity of gold clusters on titania with the appearance of nonmetallic properties. Science 281:1647–1650
20. Özbek MO, Santen RAV (2013) The mechanism of ethylene epoxidation catalysis. Catal Lett 143:131–141
21. Yang LJ, Zhou S, Ding T, Meng M (2014) Superior catalytic performance of non-stoichiometric solid solution $Ce_{1-x}Cu_xO_2$-delta supported copper catalysts used for CO preferential oxidation. Fuel Process Technol 124:155–164
22. Maiti M, Sadhukhan D, Thakurta S, Zangrando E, Pilet G, Signorella S, Bellu S, Mitra S (2014) Catalytic efficacy of copper (II)- and cobalt (III)-Schiff base complexes in alkene epoxidation. Bull Chem Soc Jpn 87:724–732
23. Ding X, Yang J, Hou JG, Zhu Q (2005) Theoretical study of molecular nitrogen adsorption on Au clusters. J Mol Struct (Theochem) 755:9–17
24. Zhou J, Li ZH, Wang WN, Fan KN (2006) Density functional study of the interaction of carbon monoxide with small neutral and charged sliver clusters. J Phys Chem A 110:7167–7172
25. Cao Z, Wang J, Zhu J, Wu W, Zhang Q (2002) Static polarizabilities of copper clusters monocarbons Cu_nCO (n=2-13) and selectivity of CO adsorption on Copper Clusters. J Phys Chem B 106:9649–9654
26. Wu L, Senapati L, Nayak SK, Selloni A, Hajaligol M (2002) A density functional study of carbon monoxide adsorption on small cationic, neutral, and anionic gold clusters. J Chem Phys 117:4010–4015
27. Neumaier M, Weigend F, Hampe O, Kappes MM (2008) Binding energy and preferred adsorption sites of CO on gold and silver-gold cluster cations: adsorption kinetics and quantum chemical calculations. Faraday Discuss 138:393–406
28. Neumaier M, Weigend F, Hampe O, Kappes MM (2006) Reactions of mixed silver-gold cluster cations AgmAun+(m+n=4,5,6) with CO: radiative association kinetics and density functional theory computations. J Chem Phys 125:104308
29. Joshi AM, Tucker MH, Delgass TKT (2006) CO adsorption on pure and binary-alloy gold clusters: a quantum chemical study. J Chem Phys 125:194707
30. Acioli PH, Burkland S, Srinivas S (2012) An exploration of the potential energy surface of the seven atom silver cluster and a carbon monoxide ligand. Eur Phys J D 66:215
31. 31 Frisch MJ, Trucks GW, Schlegel HB et al. (2009) Gaussian 09, Gaussian Inc, Pittsburgh, PA
32. Perdew JP, Chevary JA, Vosko SH, Jackson KA, Pederson MR, Singh DJ, Fiolhais C (1992) Atoms, molecules, Atoms, molecules, solids, and surfaces–Applications of the generalized gradient approximation for exchange and correlation. Phys Rev B 46:6671–6687
33. Andrae D, Haussermann U, Dolg M, Stoll H, Preuss H (1990) Energy–adjusted abinitio pseudopotentials for the 2nd and 3rd row transition–elements. Theor Chim Acta 77:123–141
34. Zhao S, Lu WW, Yun-Lai R, Yun-Li R, Wang J, Yin WP (2012) Density functional study of NO_x binding on small Au_nCu_m (n+m≤5) clusters. Comput Theor Chem 993:1039–1048
35. Foster JP, Weinhold F (1980) Natural hybrid orbitals. J Am Chem Soc 102:7211–7218
36. Dapprich S, Frenking G (1995) Investigation of donor-acceptor interactions: a charge decomposition analysis using fragment molecular orbitals. J Phys Chem 99:9352–9362
37. Frenking G, Fröhlich N (2000) The nature of bonding in transition-metal compounds. Chem Rev 100:717–774
38. Zhao S, Lu WW, Yun-Lai R, Yun-Li R, Wang J, Yin WP (2012) Density functional study of NO_x binding on small Au_nCu_m (n+m≤5) clusters. Comput Theor Chem 993:90–96
39. Sadek MM, Wang L (2006) Effect of adsorption site, size and composition of Pt/Au bimetallic clusters on the CO frequency: a density functional theory theory. J Phys Chem A 110: 14036–14042
40. Fernandez EM, Soler JM, Garzon IL, Balbas LC (2004) Trends in the structure and bonding of noble metal clusters. Phys Rev B 70:165403
41. Wesendrup R, Hunt T, Schwerdtfeger P (2000) Relativistic coupled cluster calculations for neutral and singly charged Au_3 clusters. J Chem Phys 112:9356–9362
42. Autschbach J, Siekierski S, Seth M, Schwerdtfeger P, Schwarz WHE (2002) Dependence of relativistic effects on electronic configuration in the neutral atoms of d- and f-block elements. J Comput Chem 23:804–813
43. Zhang X, Ding X, Fu Q, Yang J (2008) Theoretical study of molecular nitrogen adsorption on W_n clusters. J Mol Struct (Theochem) 867:17–21
44. Lei XL (2010) Theoretical study of small Mo clusters and molecular nitrogen adsorption on Mo clusters. Chin Phys B 19:107103
45. 45 Huber KP, Herzberg G (1979) Molecular spectra and molecular structure. IV. Constants of diatomic molecules. Reinhold, New York
46. Davidson ER, Kunze KL, Machado FB, Chakravorty S (1993) The transition-metal carbonyl bond. Acc Chem Res 26:628–635
47. Bagus PS, Hermann K, Bauschlicher CW (1984) On the nature of the bonding of the lone pair ligands to small metal-clusters. Ber Bunsen-Ges Phys Chem 88:302–303
48. Koutecky J, Pacchioni G, Fantucci P (1985) Sigma-Pi-contributions in metal-CO bond: a theoretical-study of RhCO and PdCO. Chem Phys 99:87–101
49. Baerends EJ, Rozendaal A (1986) In: Veillard A (ed) Quantum chemistry: the challenge of transition metals and coordination chemistry. Reidel, Dordrecht
50. Muller W, Bagus PS (1985) Vibrations of CO chemisorbed on metal-surfaces: cluster model studies. J Vac Sci Technol 3:1623–1626
51. Boys SF, Bernadi F (1970) Calculation of small molecular interactions by differences of separate total energies-some procedures with reduced errors. Mol Phys 10:553–556
52. 52 Mogi K, Sakai Y, Sonoda T, Xu Q, Souma Y (2003) Geometries and electronic structures of group 10 and 11 metal carbonys cations, $[M(CO)_n]^{x+}$ (M^{x+}=Ni^{2+}, Pd^{2+}, Pt^{2+}, Cu^+, Ag^+, Au^+; n=1-4). J Phys Chem A 107:3812–3821